

Numerical Solutions of the Radiosity's Equation for Low Reflectivity and Emissivity on Planet Mars

Yajni Warnapala¹ and Quiyang Deng²

Department of Mathematics, Roger Williams University
Bristol, Rhode Island 02809-2921, USA

Abstract: In this paper, the Galerkin method is used to numerically solve the exterior boundary value problem for the Radiosity equation for a spherical shape, specifically the Spherical Rhombus. The Radiosity equation is a mathematical model for the brightness of a collection of one or more surfaces when their reflectivity and emissivity are given. On planet Mars the surface emissivity is closely related to its surface temperature. The Radiosity of a surface is the rate at which the energy leaves that surface; it includes the energy emitted by a surface as well as the energy reflected from other surfaces.

Keywords: Radiosity Equation, Galerkin Method, Reflectivity, Emissivity.

I. INTRODUCTION

The mathematical model for the brightness of a collection of surfaces when their reflectivity and emissivity are known is given by the Radiosity Equation,

$$u(P) - \frac{\rho(P)}{\pi} \int_S u(Q)G(P, Q)V(P, Q)dS_Q = E(P), P \in S$$

in an exterior domain. This is a Fredholm integral equation of the second kind. Common methods such as the Adomian Decomposition Method and the Modified Decomposition Method do not work as a method of solution as this is a nonlinear singular Fredholm Equation of the second kind. Here $u(P)$ is the Radiosity or simply the brightness at P and emissivity is given by $E(P)$ and the reflectivity $\rho(P)$ is between zero and one. The assumption on the surfaces is that they are Lambertian diffuse reflectors.

Atkinson and Chien [3] did study the Radiosity equation for occluded surfaces using the Collocation method. Voigt, Hanssen and Weichmann [11] solved the Radiosity equation by an adaptive Finite Element Method and linked it to heat conduction. In 2006 Atkinson had numerical results on the planar Radiosity equation and on a matrix-vector multiplication method [3].

The Spherical Rhombus and the Spherical Cone are shapes that are controlled by two parameters. There are some numerical issues in this type of an analysis; because of the singularity in the Kernel of the integral

equation. The Kernel G which is bounded when the surface is smooth is given by $G(P, Q) = [\cos\beta_p \times \cos\beta_Q] / |(P - Q)^2|$ where β_p is the angle between n_p and $(Q - P)$. The formula for the Spherical Rhombus shape is given by:

$$\begin{aligned} x &= \cos(0.5\mu)\sin(0.5\mu)\sin(\mu)\cos(\beta) \\ y &= \sin(0.5\mu)\cos(0.5\mu)\sin(\mu)\sin(\beta) \\ z &= \cos(\beta) \end{aligned}$$

and the formula for the Spherical Cone shape is given by:

$$\begin{aligned} x &= \cos(0.5\mu)\sin(\mu)\sin(\mu)\cos(\beta) \\ y &= \sin(\mu)\sin(\beta) \\ z &= \sin(0.5\mu)\cos(\mu) \end{aligned}$$

where β varies from zero to π while μ will vary from zero to 2π . The Radiosity equation, which is a mathematical model for the brightness of a collection of one or more surfaces when their reflectivity and emissivity are given, is used in many diffusion problems. One practical value of all these computations can be with the inside lighting (brightness) of a space craft that one day might land on planet Mars. We researched the feasibility of obtaining good convergence results for the Spherical Rhombus and the Spherical Cone surfaces for the Dirichlet boundary condition. It is our view that smaller reflectivity values would reduce computational costs associated with obtaining Galerkin coefficients. Also as the Mars atmosphere is less volatile and less diverse than the Earth's atmosphere, constant emissivity functions would be more appropriate for testing. We used the Green's theorem to solve the integral equation on the boundary of the surface for the Dirichlet problem. Previously, multiple surfaces were used to test this method for the Dirichlet condition, such as the sphere, the ellipsoid, and the oval of Cassini (Warnapala, 2013) [12]. The shapes we are working on are slowly reaching a more realistic shape that is simply connected and bounded and can be a part of a space craft that is suitable for the brightness that exists on planet Mars. The Exterior Boundary problem for all these surfaces will be solved using the Gaussian Quadrature Method, where rotations of the coordinates would be used to minimize the inherent singularity that is present in the fundamental solution of the Radiosity equation. The

Boundary condition will only take into account the reflection and absorption of the incoming light waves. The assumption on the surfaces is that they are Lambertian diffuse reflectors. Brightness of these surfaces are the same regardless of the observer's angle of view, thus they obey the Lambert's Cosine Law or are isotopic.

II. PRELIMINARY THEORETICAL BACKGROUND

S is a closed bounded surface in \mathbb{R}^3 and it belongs to the class of C^2 . D_+ denotes the exterior of S . Then the Radiosity Equation from computer graphics is given by

$$u(P) - \frac{\rho(P)}{\pi} \int_S u(Q)G(P,Q)V(P, Q)dS_Q = E(P), P \in S \tag{2.1}$$

with E a given emissivity function. E is l times continuously differentiable and the l^{th} order derivatives of the surface representations are also Holder continuous with exponent λ . The function spaces we are working with are $L^2(S)$ and $C(S)$, the square-integrable Lebesgue measurable functions and the continuous functions on S , respectively.

A. Formulation of the Integral of the Second Kind

The boundary value problem was reformulated as an integral equation.

$$u(P) - \int_S u(Q) \frac{\partial(G(P, Q))}{\partial v_Q} d\sigma_Q \text{ with } P \notin D_+ \tag{2.2}$$

where $r = |P - Q|$.

The kernel $G(P, Q)$ is given by

$$G(P, Q) = \frac{[(Q - P) \cdot n_P][(P - Q) \cdot n_Q]}{|P - Q|^4} \tag{2.3}$$

Here n_p is the inner unit normal to S at P , and $V(P, Q) = 1$ (assumption is that the points P and Q are in a straight line and does not intersect the surface at any other point), an unclouded surface.

Here $Y_n^m, n = -m, \dots, m$ denote the basis functions that are the linearly independent spherical harmonics of order m given by

$$Y_n^m(\phi, \theta) = \left(\frac{1}{2\pi}\right)^{1/2} \left(m + \frac{1}{2}\right)^{1/2} \frac{(m-n)!}{(m+n)!} p_n^m(\cos \theta) e^{im\phi}$$

$$u(P) - \int_S u(Q) \frac{\partial G(P, Q)}{\partial v_Q} d\sigma_Q = E(P), P \in S \tag{2.4}$$

The integral equation is given by

$$\mathbf{u} - \mathbf{K}\mathbf{u} = \mathbf{E} \text{ where } \mathbf{K}\mathbf{u}(P) = \int_S u(Q) \frac{\partial}{\partial v_Q} \left(\frac{[(Q-P) \cdot n_P][(P-Q) \cdot n_Q]}{\pi |P-Q|^4} \right) d\sigma_Q \tag{2.5}$$

By the assumptions on $G(P, Q)$ the kernel $\frac{\partial \Psi(P, Q)}{\partial v_Q}$ is bounded on $S \times S$, and is compact from

$C(S)$ to $C(S)$ and $L^2(S)$ to $L^2(S)$.

B. Basis Functions

The Legendre basis function $p_n(\cos \theta), p_n^m(\cos \theta) \cos(m\phi), p_n^m(\cos \theta) \sin(m\phi), 1 \leq m \leq n$, are spherical harmonics of degree n . For $0 \leq n \leq N$, the total number of basic functions is $d(N) = (N + 1)^2$ and $p_n^m(t) = (-1)^m (1 - t^2)^{m/2} \frac{d^m}{dt^m} P_n(t)$. If $\mu \in C^{l,\lambda}(u)$, then there is a sequence of spherical polynomials T_N of degree $\leq N$ for which $\|\mu - T_N\|_\infty \leq \frac{C}{N^{l+\lambda}}, N \geq 1$. The spherical polynomials are dense in both $C(U)$ and $L^2(U)$. Let $P_N \mu$ denote the partial sum of the Laplace series of μ restricted to terms of degree $\leq N$. On $L^2(U), P_N$ is orthogonal and $\|P_N\|_2 = 1$. On $C(U), \|P_N\|_\infty = (\sqrt{\frac{8}{\pi}} + \partial_N) \sqrt{N}$, with $\partial_N \rightarrow 0$. If $\mu \in C^{l,\lambda}(U)$, then $\|\mu - P_N \mu\| \leq \frac{C_l}{N^{l+\lambda-1/2}}$.

III. THE GALERKIN METHOD

The variable of integration in (2.6) was changed converting it to a new integral equation defined on the unit sphere U . The Galerkin method was applied to this new equation, using spherical polynomials to define the approximating subspaces.

$m : U \rightarrow_{onto}^{1-1} S$, where m is at least differentiable, for which the following properties are satisfied.

$$E \in C^{l,\lambda}(S) \text{ and } S \in C^{l+1,\lambda} (S \in C^2 \text{ for } l = 0) \text{ implies } \hat{E} \in \mathcal{G}^{l,\lambda}(U), \tag{3.1}$$

$$\hat{E}(Q) = E(m(Q)), Q \in U. \tag{3.2}$$

By changing the variable of integration in (2.6) we obtained the new equation over U .

$$(I - K)\hat{u} = \hat{E}, \hat{E} \in \mathcal{G}(U) \tag{3.3}$$

where $\mathbf{K}(P, Q) = \frac{\rho(P)}{\pi} G(P, Q)V(P, Q)$.

The notation $\hat{\cdot}$ denotes the change of variable from S to U , as in (3.2). The operator $(I - K)^{-1}$ exists and is bounded on $C(U)$ and $L^2(U)$. The dimension of the approximating subspace of spherical polynomials of degree $\leq N$ is $d = (N + 1)^2$: and we let $\{h_1, \dots, h_d\}$ denote the basis of spherical harmonics Galerkin's method for solving (3.3) is given by

$$(I - P_N \hat{K}) \hat{u}_N = P_N \hat{E} \quad (3.4)$$

The solution is given by $\hat{u}_N = \sum_{j=1}^d \alpha_j h_j$.

$$\alpha_i (h_i, h_i - \sum_{j=1}^d \alpha_j (\hat{K} h_j, h_i)) = (\hat{E}, h_i) \quad i = 1, \dots, d. \quad (3.5)$$

The convergence of u_N to u in $L^2(S)$ is straightforward.

A. Calculation of the Galerkin Coefficients

The coefficients $(\hat{K} h_j, h_i)$ are fourfold integrals with a singular integrand. To calculate $\hat{K} h_j$ we first rotated the surface S such that \hat{p} is not a singular point internal to the integration region $[0, \pi] \times [0, 2\pi]$ ([2]). Because the Galerkin coefficients $(\hat{K} h_j, h_i)$ depends only on the surface S we calculated them separately for $N \leq N_{max}$.

IV. EMISSIVITY AND REFLECTIVITY ON PLANET MARS

To construct the inside part of a space craft with the correct brightness, it is important to discuss the reflectivity and emissivity from what we know of the atmosphere on Mars. Compared with Earth, Mars has lower surface temperatures and much lower atmospheric absorption and radiation and also has higher surface emissivity. The atmospheric emission from oxygen and water vapor is almost negligible due to very low atmospheric density and optical depth. There are three types of radio noise emissions on Mars. Martian surface emissivity is closely related to physical temperature and materials on Mars. The air on Mars is quite dry and effects from rain can be neglected. The mass density on Mars is 61 times than that of Earth due to low pressure. Mars has a large surface emissivity due to the land surfaces having lower dielectric constants. No water surface has been detected on Mars. The soil's moisture and surface roughness also affect the emissivity. Lower material densities have lower reflectivity. Emissions include cosmic and galactic noise. Both surface reflectivity

and emissivity have a radio frequency dependence and the emissivity coefficient increases as radio frequency increases. All in all, on average, Earth has lower value of emissivity and reflectivity. But rocks on Mars usually have lower emissivity. Mars has higher average surface emissivity due to the roughness of soil and rocks on the surface. Surface emissivity (E) is related to reflectivity an $E = 1 - \rho$, which means the sum of emissivity and reflectivity is 1.

V. NUMERICAL RESULTS

The true solution we tested is given by $u(x, y, z) = 1$. Thus we assumed $u = E$. $NINTI = 16$ are interior nodes needed for calculating $\hat{K} h_j$, $NINTE = 8$ are the exterior nodes needed for calculating $(\hat{K} h_j, h_i)$. $NDEG = 5$ is the degree of the approximate spherical harmonics, the number d of basis functions equals to $(NDEG + 1)^2$.

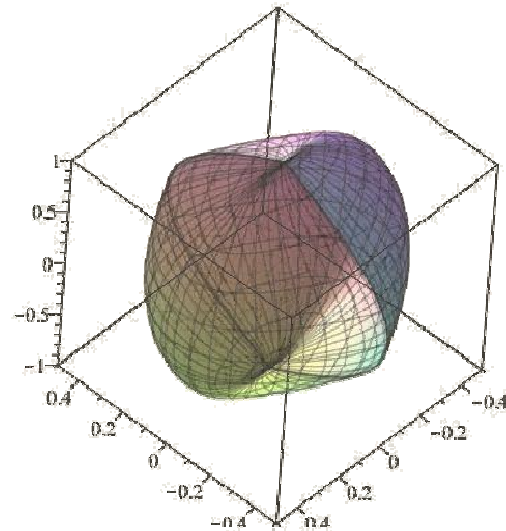


Fig. 1: Let S be a Spherical Rhombus

rho	Distance				
	(500, 200, 300)	(50, 200, 300)	(500, 20, 300)	(500, 200, 30)	(-4000, -5000, -6000)
0.08	4.838E-03	4.838E-03	4.837E-03	4.838E-03	4.837E-03
0.002	1.204E-04	1.200E-04	1.198E-04	1.203E-04	1.199E-04
0.0005	2.967E-05	2.931E-05	2.907E-05	2.961E-05	2.914E-05
0.00001	3.698E-08	3.224E-07	5.685E-07	2.645E-08	4.957E-07
0.00005	2.456E-06	2.097E-06	1.861E-06	2.393E-06	1.924E-06
5.00E-6	2.654E-07	6.248E-07	8.709E-07	3.289E-07	7.981E-07
1.00E-7	5.618E-07	9.212E-07	1.167E-06	6.252E-07	1.094E-06
1.00E-10	5.678E-07	9.272E-07	1.173E-06	6.313E-07	1.100E-06

Table 1: Convergence results for small reflectivity rho values according to the distance of the light wave from the outer boundary of the surface. This can depict one of the two following cases: The Rhombus design of an inside room of a space craft with an outer light source or it could be a stationary part of the craft that has already landed on planet Mars, in this case the light waves will originate from the atmosphere of the planet.

As one can see from the above table the direction of the light waves do not impact the convergence results. Further low reflectivity values give excellent results while slightly larger values give reasonable results. If we had increased the integration nodes we might have obtained better results for slightly larger reflectivity values as well.

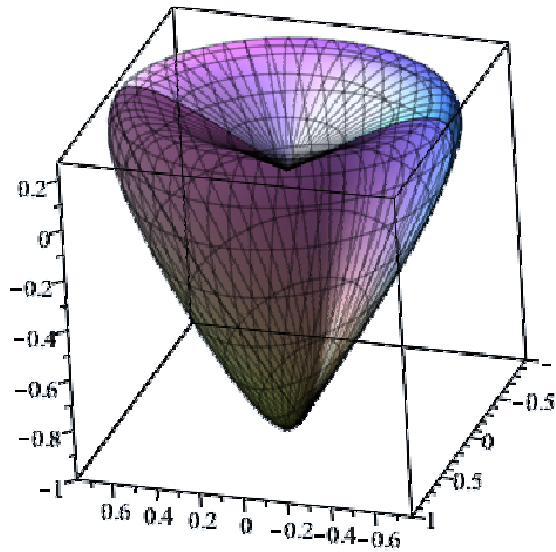
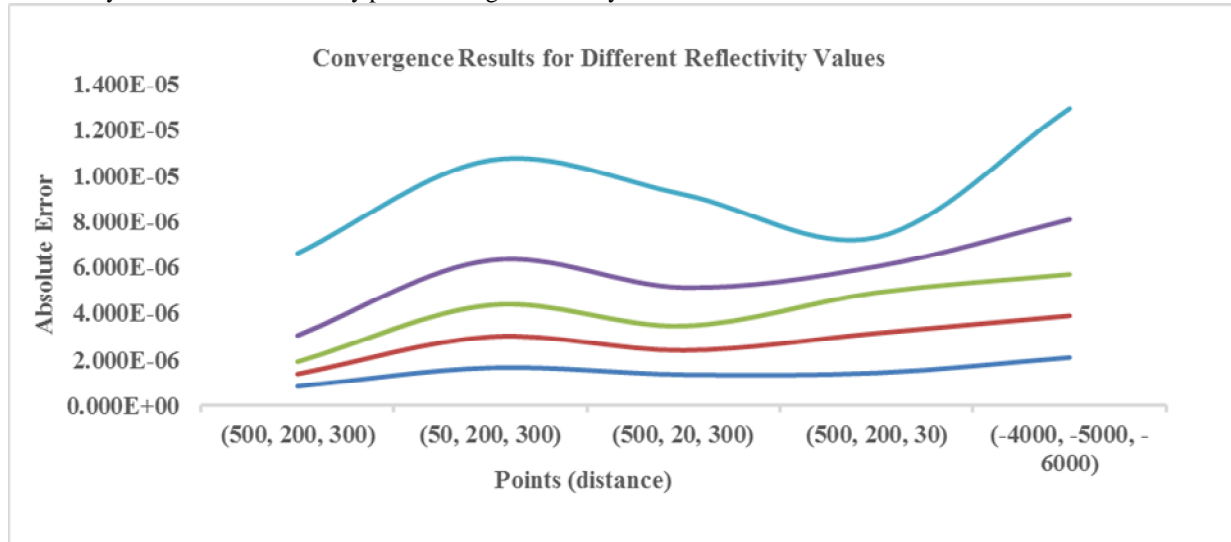


Fig. 2 Let S be a Spherical Cone

rho	Distance				
	(500, 200, 300)	(50, 200, 300)	(500, 20, 300)	(500, 200, 30)	(-4000, -5000, -6000)
0.08	4.839E-03	4.840E-03	4.840E-03	4.847E-03	4.840E-03
0.002	1.215E-04	1.223E-04	1.220E-04	1.192E-04	1.228E-04
0.0005	3.078E-05	3.159E-05	3.129E-05	2.850E-05	3.204E-05
0.00001	1.142E-06	1.955E-06	1.657E-06	1.136E-06	2.401E-06
0.00005	3.561E-06	4.374E-06	4.076E-06	1.283E-06	4.821E-06
5.00E-6	8.394E-07	1.653E-06	1.354E-06	1.428E-06	2.099E-06
1.00E-7	5.430E-07	1.356E-06	1.058E-06	1.734E-06	1.802E-06
1.00E-10	5.369E-07	1.350E-06	1.052E-06	1.740E-06	1.796E-06

Table 2: The reflectivity values (rho) vs the distance from the light source.

In the spherical cone case the smaller reflectivity values do not necessarily mean better convergence, the best convergence results were obtained when ρ the reflectivity was 0.0001 for all waves regardless of direction. From the above tables it is evident that smaller reflectivity values give better convergence results compared to slightly larger values. We can also see from the above table that when you decrease the reflectivity, the accuracy improves. Inside of space crafts are built with some form of aluminum or carbon fiber both of which have low reflectivity values. Low reflectivity produces high emissivity.



Graph 1: The absolute error is not similar for all reflectivity values regardless of the direction of the light source

From the above graph for the Spherical Rhombus, we see that for the points away from the boundary there is much greater accuracy than for points near the boundary. This is because the integrand is more singular at points near the boundary.

This is due to the following fact: the kernel function involves $1/r^2$ which is much more oscillatory when r becomes large. Therefore in this case we must increase the integration nodes to achieve the same accuracy. $NINTE < NINTI$, because the integrand of $(h_i, \hat{K}h_j)$ is smoother than the integrand of $\hat{K}h_j$. Also $NINTE \geq (NDEG + 1)$.

VI. FUTURE RESEARCH AND FINAL CONCLUSIONS

For all calculations we used Fortran 77. We conclude that the error is affected by the boundary S , boundary data, emissivity and reflectivity ρ . If we want to obtain more accuracy, we must increase the number of integration nodes for calculating the Galerkin coefficients $(\hat{K}h_j, h_i)$. The cost of calculating the Galerkin coefficients is high. When $NINTI$ or $NINTE$ are doubled, the CPU time increases by four times.

In order to eliminate more interior Neumann eigenvalues we need a more powerful computer which would decrease the CPU time considerably. For the shapes tested the convergence results were quite good, for varied values of reflectivity. In the future we plan to investigate the Neumann and Robin boundary value problems where the kernels will be much less smoother. Further we made the assumption that the incoming waves are constant or that Emissivity is

constant. In the future we plan to change the true solution to functions such as $\sin(\mu)$ or $\sin(\beta)$; the light waves that are periodic in nature. Solutions to the Radiosity equation are relevant to agencies such as NASA because of their use in energy balancing relationships in isothermal and non-isothermal surfaces and space. The Radiosity equation is generally an energy balanced equation for discrete surfaces. Prescribing the values of a given emissivity and reflectivity function on the boundary of the obstacle physically corresponds to prescribing the brightness of the light wave. Currently no numerical results or analytical results are available for the Spherical Rhombus or Spherical Cone.

ACKNOWLEDGMENT

I would like to thank Mrs. Kennedy for technical support in getting this paper ready.

REFERENCES

- [1] K. E. Atkinson, The numerical solution of the Laplace's equation in three dimensions, SIAM J. Numer. Anal., 19, (1982), pp. 263-274.
- [2] K. E. Atkinson, The Numerical Solution of Integral Equations of the Second Kind, Cambridge University Press, 1998.
- [3] K. E. Atkinson and D. Chien, A Study of the Fast Solution of the Occluded Radiosity Equation, Electronic Transactions on Numerical Analysis, Vol. 23, pp. 219-250, 2006.
- [4] David Colton and Rainer Kress, Integral equation methods in scattering theory, 1983.
- [5] J. Arvo, The Role of the Functional Analysis in Global Illumination, Rendering Techniques '95, edited by P.M. Hanrahan and W. Purgathofer, pp.115-126, Springer-Verlag, NY 1995.

- [6] R. E. Kleinman and R. Kress, On the Condition Number of Integral Equations in Acoustics using Modified Fundamental Solutions, *IMA Journal of Applied Mathematics*, (1983), 31, pp. 79-90.
- [7] T. C. Lin, The numerical solution of the Helmholtz equation using integral equations, Ph.D. thesis, (July 1982), University of Iowa, Iowa City, Iowa.
- [8] T. C. Lin, The numerical solution of Helmholtz equation for the exterior Dirichlet problem in three dimensions, *SIAM, J. Numerical Anal.*, vol 22, No. 4, pp.670-686, 1985.
- [9] T. C. Lin, Smoothness results of single and double layer solutions of the Helmholtz equations, *Journal of Integral Equations and Applications*, Vol.1, Number 1, pp. 83-121,1988.
- [10] Harry A. Schenk, Improved integral formulation for acoustic radiation problems, *Journal of the Acoustical Society of America*, (1967), pp. 41-58.
- [11] A. Voigt, N. Hanssen and C. Weichmann, The radiosity equation for solving global heat transfer in industrial furnaces, *Mathematical and Computer Modeling*, Vol. 39, Issues 2-3, pp. 145-150, Jan 2004.
- [12] Warnapala, Yajni. "Numerical Solution of the Radiosity Equation via Galerkin Method: Dirichlet Condition." *International Journal Methods and Applications* 10 (2013): 73-89. Print.